

A review from elasto- to twistocaloric cooling

Ziqian Zhang(张子千), Xiang Zhou(周湘), and Zunfeng Liu(刘遵峰)

Citation: Chin. Phys. B, 2026, 35 (**7**): 078102. DOI: 10.1088/1674-1056/ae6174
http://cpb.iphy.ac.cn; http://iopscience.iop.org/cpb

What follows is a list of articles you may be interested in

Enhancing the thermoelectric performance through the mutual interaction between conjugated polyelectrolytes and single-walled carbon nanotubes

Shuxun Wan(万树勋), Zhongming Chen(陈忠明), Liping Hao(郝丽苹), Shichao Wang(王世超), Benzhang Li(李本章), Xiao Li(黎潇), Chengjun Pan(潘成军), and Lei Wang(王雷)
Chin. Phys. B, 2022, 31 (**2**): 028104. DOI: 10.1088/1674-1056/ac48f9

Moisture-sensitive torsional cotton artificial muscle and textile

Yuanyuan Li(李媛媛), Xueqi Leng(冷雪琪), Jinkun Sun(孙进坤), Xiang Zhou(周湘), Wei Wu(兀伟), Hong Chen(陈洪), Zunfeng Liu(刘遵峰)
Chin. Phys. B, 2020, 29 (**4**): 048103. DOI: 10.1088/1674-1056/ab7745

Universal properties of relaxation and diffusion in condensed matter

K L Ngai(倪嘉陵)
Chin. Phys. B, 2017, 26 (**1**): 018105. DOI: 10.1088/1674-1056/26/1/018105

Fabrication and formation mechanism of closed-loop fibers by electrospinning with a tip collector

Xu Yan(闫旭), Miao Yu(于淼), Wen-Peng Han(韩文鹏), Ming-Hao You(犹明浩), Jun-Cheng Zhang(张君诚), Rui-Hua Dong(董瑞华), Hong-Di Zhang(张红娣), Yun-Ze Long(龙云泽)
Chin. Phys. B, 2016, 25 (**7**): 078106. DOI: 10.1088/1674-1056/25/7/078106

Progress in organic spintronics

Yang Fu-Jiang (杨福江), Han Shi-Xuan (韩士轩), Xie Shi-Jie (解士杰)
Chin. Phys. B, 2014, 23 (**5**): 058106. DOI: 10.1088/1674-1056/23/5/058106

TOPICAL REVIEW — Multiferroicity and multicaloric effects

A review from elasto- to twistocaloric cooling

Ziqian Zhang(张子千)[1], Xiang Zhou(周湘)[2,†], and Zunfeng Liu(刘遵峰)[1,‡]

[1] *State Key Laboratory of Medicinal Chemical Biology, College of Chemistry and College of Pharmacy, Key Laboratory of Functional Polymer Materials, Frontiers Science Center for New Organic Matter, Nankai University, Tianjin* 300071, *China*
[2] *Department of Science, China Pharmaceutical University, Nanjing* 211198, *China*

(Received 24 December 2025; revised manuscript received 8 April 2026; accepted manuscript online 20 April 2026)

As a significant branch of solid-state cooling, elastocaloric and twistocaloric cooling achieve reversible temperature changes through the mechanical deformation of functional materials. Compared to vapor-compression refrigeration, they have emerged as promising alternatives because of high efficiency, environmental compatibility, and structural flexibility. Among various cooling strategies, twistocaloric cooling has recently attracted growing attention owing to its large temperature changes under low driving stress through torsional deformation. Here, we summarize recent progress in flexible twistocaloric and elastocaloric materials and devices, covering shape memory alloys, elastomeric polymers, and other emerging polymers. We elucidate the cooling mechanisms from molecular levels and compare the cooling properties among kinds of cooling materials. Then, large- and small-scale cooling devices driven by twisting, uniaxial stretching, and hybrid deformation are clarified, and critical discussions on heat-transfer efficiency, mechanical stability, and scalability are emphasized. Finally, key challenges and future opportunities are outlined from material optimization, device engineering and multi-mode integration, and theoretical modeling perspectives, highlighting pathways toward compact, durable, and energy-efficient solid-state cooling technologies.

Keywords: twistocaloric cooling, elastocaloric cooling, cooling materials and devices

PACS: 81.05.Lg, 65.40.De, 07.20.Mc, 84.60.Rb

DOI: 10.1088/1674-1056/ae6174 **CSTR:** 32038.14.CPB.ae6174

1. Introduction

The rapidly increasing demand for cooling in buildings, electronic systems, and individuals has placed growing pressure on energy infrastructure worldwide.[1–3] With the global stock of air-conditioning units exceeding 1.6 billion and cooling already accounting for nearly 20% of global electricity consumption, further increases in cooling demand are expected in the coming decades.[4,5] However, the efficiency of conventional vapor-compression refrigeration is approaching its thermodynamic ceiling, leaving limited room for substantial performance improvement through incremental system optimization.[6,7] Solid-state cooling has therefore emerged as a promising alternative, leveraging phase transition and entropy modulation in functional materials to achieve fast, reversible, and gas-free temperature changes.[8–11] Among the various cooling strategies, mechanically driven twistocaloric and elastocaloric effects are particularly appealing for flexible and miniaturized cooling platforms, which directly couple mechanical deformation with thermal response and are implemented in fiber-, ribbon-, or membrane-based structures.[12–15]

Recent studies have demonstrated that a wide range of flexible materials can exhibit pronounced elastocaloric or twistocaloric effects.[16–18] Shape memory alloys (SMAs), particularly NiTi-based SMAs, remain the most powerful candidates due to their large latent heat and excellent mechanical properties.[19,20] Microstructural engineering strategies, such as gradient structures, doping, and secondary-phase reinforcement, have further improved their cooling efficiency, reduced hysteresis, and enhanced fatigue resistance.[21,22] In parallel, elastomeric polymers, including natural rubber (NR), SEBS copolymers, and thermoplastic polyurethanes (TPUs), offer entropy-driven elasticity, large reversible strain, and relatively low driving stress.[23–25] Torsional deformation has further expanded the accessible cooling window of these polymers by activating large entropy changes at substantially reduced strain to realize lightweight and mechanically compliant designs.[26,27] Additional polymer systems (including ferroelectric polymers, rigid-chain fibers, and spin-crossover composites) reveal new directions for molecular design.[28–30]

Progress in flexible cooling devices has evolved alongside material development.[31] Uniaxial stretching-based devices established the feasibility of the elastocaloric effect but were limited in deformation strokes and inefficient in heat transfer.[32] In contrast, twisting-based cooling devices exploit radial shear-stress gradients and more uniform deformation fields to achieve high cooling efficiency under lower driving forces, facilitating compact and scalable de-

†Corresponding author. E-mail: zhouxiang@cpu.edu.cn
‡Corresponding author. E-mail: liuzunfeng@nankai.edu.cn

© 2026 Chinese Physical Society and IOP Publishing Ltd. All rights, including for text and data mining, AI training, and similar technologies, are reserved.

vice architectures.[33,34] More recently, hybrid deformation modes that combine stretching, twisting, bending, or contact-separation processes have been introduced to enhance heat-transfer efficiency and reduce actuation requirements, enabling continuous-flow cooling and higher power density.[35]

Despite these advances, a comprehensive understanding linking material structure, deformation mode, entropy modulation, and device performance remains incomplete. Existing reviews have focused on either material properties and fundamentals or device architectures and designs, but seldom integrate both perspectives to reveal the relationships among structure, mechanism, and performance. This review therefore provides a systematic framework that bridges twistocaloric and elastocaloric materials with flexible solid-state cooling device architectures, highlighting key deformation principles, material design strategies, device-level engineering, and emerging opportunities for intelligent, low-energy thermal-management technologies.

2. Properties of flexible cooling materials

The cooling behavior of flexible solid-state materials is dictated by their phase-transition or entropy-modulation mechanisms, deformation modes, and microstructural responses. Shape memory alloys exploit martensitic transformations to deliver a large adiabatic temperature drop, whereas elastomeric polymers rely on entropy-driven chain alignment; both of them exhibit enhanced cooling performance under torsional loading. Additional polymer systems (including ferroelectric, rigid-chain, and spin-crossover composites) provide complementary cooling pathways through dipole, conformational, or spin-state rearrangements. The following subsections outline representative materials in each class and discuss their cooling behaviors in relation to their molecular structure, deformation modes, and entropy-modulation pathways.

2.1. Shape memory alloys

SMAs, particularly NiTi-based SMAs, are among the most promising elastocaloric materials owing to the large latent heat associated with the B2↔B19′ martensitic transformation (Fig. 1(a)).[36] This transformation enables pronounced adiabatic temperature changes and high energy-conversion efficiency.[37] Specifically, the cooling effect in NiTi-based SMAs originates from the stress-induced martensitic transformation and the associated entropy changes. Upon the application of external stress, the material undergoes a structural transition from the high-symmetry cubic austenite phase (B2) to the low-symmetry monoclinic martensite phase (B19′), a process that drives the system toward a lower-entropy state and triggers the release of latent heat, thereby increasing the material's temperature. Subsequently, during the adiabatic unloading process, the material experiences a reverse transformation to the high-entropy austenitic state; this process necessitates the absorption of substantial latent heat, resulting in a significant drop in the material's temperature and enabling high-performance solid-state cooling. For example, Takeuchi *et al.* reported a ΔT_{ad} of −17.0 K in 3-mm-diameter NiTi wires during recovery from 8.5% tensile strain, achieving a COP of 11.8 and a specific work of 78 MJ·m^{-3}, which was approximately six times higher than that of conventional vapor-compression refrigerants.[38]

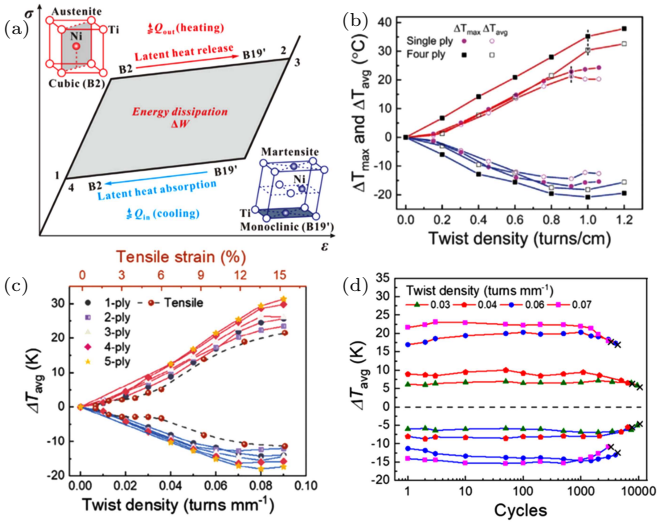


Fig. 1. Cooling properties of NiTi-based SMAs. (a) Molecular mechanisms of elastocaloric and twistocaloric effects of NiTi-based SAMs. Reproduced with permission from Ref. [36] Copyright 2021 Elsevier. (b) Maximum and surface-average temperature changes of single-ply and four-ply NiTi wires with various twist density at 0% strain. Reproduced with permission from Ref. [24] Copyright 2019 The American Association for the Advancement of Science. (c) ΔT_{avg} of NiTi wires (from 1-ply to 5-ply) as a function of twist density. (d) Cycle stability of NiTi wires under various twist densities. Reproduced with permission from Ref. [33] Copyright 2024 Wiley-VCH.

However, uniaxial tension demands a high driving stress and large mechanical setups, and suffers from significant hysteresis and fatigue, which limit its applicability. Recent studies have shown that torsional loading can overcome these issues by generating a nonlinear radial stress gradient that activates phase transformation more efficiently under lower stress.[27,39] The Liu group achieved a ΔT_{ad} of −17.0 K in single $Ni_{51.3}Ti_{48.7}$ wires and −20.8 K in four-wire bundles during isometric untwisting (Fig. 1(b)).[24] When combining untwisting with tensile unloading, an average cooling of −12.1 K and a COP of 8.5 were obtained. Further, they demonstrated a ΔT_{ad} of −18.0 K using five-wire bundles (Fig. 1(c)) and an exceptional COP of 30.8 (≈ 82% of the Carnot limit).[33] Importantly, the torsion-induced periodic nonlinear stress distribution suppressed crack initiation and delayed fatigue, enabling over 14752 stable cycles (Fig. 1(d)). Additional work on NiTi rods and bent NiTi wires (ΔT_{ad} up to −15.0 K and −11.3 K, respectively) further highlights the advantages of torsion over bending and tension. The latter often produces incomplete phase transformation or excessive hysteresis.[40,41]

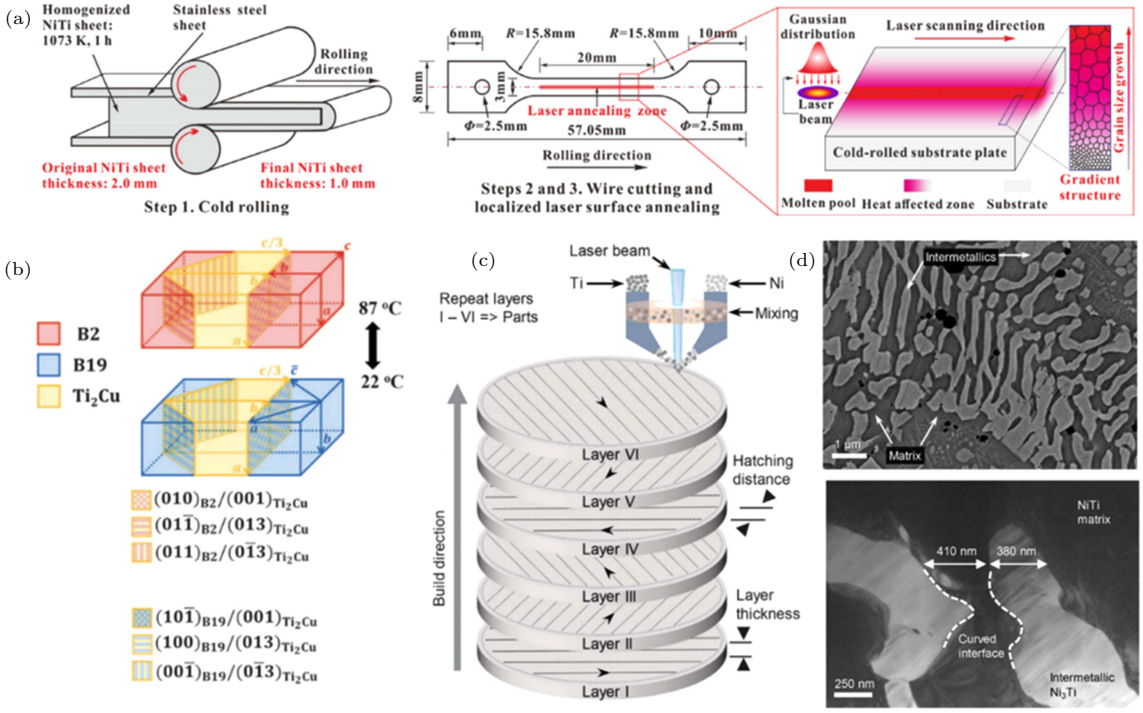


Fig. 2. The method of modifying NiTi-based SMA to increase fatigue durability. (a) Gradient grain size ranging from approximately 10 mm to 3500 mm induced by laser local annealing. Reproduced with permission from Ref. [49] Copyright 2021 Elsevier. (b) For Cu-doped $Ti_{54}Ni_{34}Cu_{12}$ alloy, Ti_2Cu phase enhanced the compatibility of the conversion interface. Reproduced with permission from Ref. [51] Copyright 2015 The American Association for the Advancement of Science. (c) $Ni_{51.5}Ti_{48.5}/Ni_3Ti$ composite nano-precipitated phase alloy made by additive manufacturing. (d) Scanning electron microscopy (SEM) image and bright-field transmission electron microscopy (TEM) image. Typical curved interfaces were delineated. Reproduced with permission from Ref. [53] Copyright 2019 The American Association for the Advancement of Science.

Despite their excellent cooling potential, traditional NiTi SMAs still suffer from large hysteresis and limited fatigue life.[42] Several microstructural engineering strategies have therefore been pursued.[43–47] The refinement of grains to the nanoscale has emerged as an effective strategy for minimizing frictional dissipation during martensitic transformations, thereby enhancing cooling performance. Specifically, the fabrication of nanocrystalline NiTi alloys with a grain size of 4 nm enables an exceptionally low stress hysteresis of 6.3 MPa even under a high strain of 5%. This microstructural optimization facilitates a maximum ΔT_{ad} of -11.4 K and achieves a COP of 11.8.[48] Gradient-structure NiTi fabricated by localized laser annealing (Fig. 2(a)) exhibited an 83% increase in COP compared with coarse-grained NiTi, achieving a ΔT_{ad} of -13.6 K at 4% strain recovery with a reduced hysteresis of 60 MPa.[49] Post-deformation annealing enabled PDAGS-NiTi with a ΔT_{ad} of -12.4 K and a COP of 42 while reducing energy dissipation by 77% and maintaining stable superelasticity over 100 cycles.[50] Alloy doping has also proven effective, such as Cu (Fig. 2(b)).[51] For example, nanocrystalline $Ti_{50}Ni_{42}Cu_6Fe_2$ wires achieved a temperature span of ~ 28 K with an average hysteresis of only 180 MPa.[52] Introducing a reinforcing intermetallic phase in NiTi/Ni_3Ti nanocomposites produced quasi-linear stress–strain behavior (80–90 GPa), yielding a ΔT_{ad} of -4.1 K and a Carnot-normalized COP seven times that of cast NiTi (Fig. 2(c)).[53] These strategies collectively enhance stiffness, load transfer, and resistance to dislocation motion, offering viable pathways toward fatigue-resistant NiTi elastocaloric materials (Fig. 2(d)).

Beyond NiTi alloys, copper- and cobalt-based SMAs provide additional advantages, including high thermal conductivity, large temperature spans, and small stress hysteresis.[54,55] Single-crystal $Cu_{70.5}Al_{17.5}Mn_{12}$ exhibited a ΔT_{ad} of -8.4 K during unloading from 10% strain,[56] while polycrystalline $Cu_{71}Al_{18}Mn_{11}$ microwires produced a ΔT_{ad} of -5 K under 150 MPa.[57] Subsequently, grain-engineered bamboo-like $Cu_{71.1}Al_{17.2}Mn_{11.7}$ microwires further increased the ΔT_{ad} to -11.9 K.[58] Using a similar fabrication route, $Co_{49}Ni_{21}Ga_{30}$ microwires achieved a ΔT_{ad} of -4.1 K.[59] These emerging results demonstrate that non-NiTi SMAs, despite lower entropy change, offer complementary advantages such as lower driving stress and broader operational temperature ranges.

2.2. Elastomeric polymers

Elastomeric polymers have recently gained attention as promising candidates for flexible solid-state cooling owing to their entropy-driven elasticity, large reversible strain, and low driving stress.[60,61] The rapid and reversible temperature changes of elastomeric polymers during loading and unloading can be directly observed through infrared thermal imaging technology (Fig. 3(a)).[62] At the molecular level, the cooling mechanism is fundamentally driven by the change in confor-

mational entropy of the polymer chains. Initially, the elastomer consists of randomly coiled molecular chains with a high degree of disordered configurations, representing a high-entropy state. Upon the application of external stress (such as uniaxial stretching or twisting), the molecular chains are forced to align along the direction of the applied load, leading to a sharp decrease in entropy. This reduction in entropy triggers the release of thermal energy, causing the increase of the material's temperature. When the external stress is removed, the aligned chains spontaneously recoil to their original disordered state. This rapid increase in entropy necessitates the absorption of heat and results in a pronounced and reversible cooling effect, realizing high reversibility, minimal hysteresis, and excellent fatigue resistance. For example, a 650 μm NR foil achieved a ΔT_{ad} of −10.3 K upon recovery from 700% tensile strain and delivered a COP of ∼ 6.9 at a pre-strain of 300%.[63] With a 10% enhancement in heat-exchange efficiency, the NR blend of 20 %wt ground tire rubber yielded ΔT_{ad} up to −12.8 K and a COP of 3.8.[64]

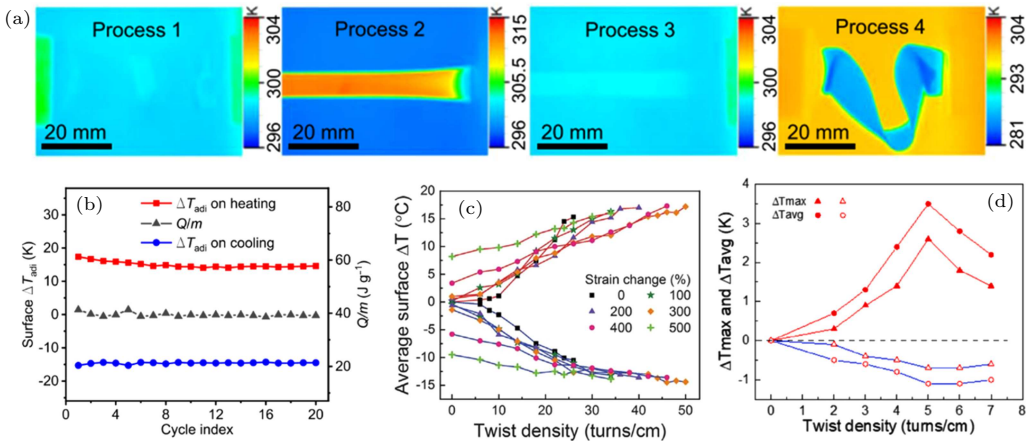


Fig. 3. Cooling properties of elastomeric polymers and PBO fibers. (a) Infrared thermal images showed the temperature changes of elastomer polymers during the loading and unloading process. (b) Surface ΔT_{ad} evolution of TPEs-1 during 20 times cycles with 600% strain. Reproduced with permission from Ref. [62] Copyright 2022 Springer Nature. (c) ΔT_{avg} as a function of twist density in supercoiled NR fibers under different tensile strains (0–500%). Reproduced with permission from Ref. [24] Copyright 2019 The American Association for the Advancement of Science. (d) ΔT_{max} and ΔT_{avg} as a function of twist density in self-coiled PVDF fibers. Reproduced with permission from Ref. [28] Copyright 2021 Elsevier.

However, NR suffers from several intrinsic limitations, including restricted fatigue life under extreme deformation and relatively low thermal conductivity, which collectively constrain its efficiency in practical cooling systems.[65] Researchers have explored alternative polymeric elastomers with reduced mechanical dissipation, tunable molecular architectures, and improved processability, including SEBS copolymers, thermoplastic polyurethanes (TPUs), and so on. Owing to their uniform chain architectures and reversible conformational transitions, SEBS-based materials can deliver large ΔT_{ad} values (such as −15.3 K and −16.3 K) and excellent COP (15.7 and 16.2, respectively).[62,66] After 20 cycles under a tensile strain of 600%, the ΔT_{ad} and heat transfer capacity remain stable (Fig. 3(b)). TPU-based fibers and films exhibit ΔT_{ad} of −3.5 K to −8 K at strains around 400%–500%,while maintaining stable performance over multiple cycles.[67,68] Importantly, their compatibility with melt processing and 3D printing enables precise structural design and facilitates integration into prototype cooling devices.

In spite of these advances, the uniaxial stretching-driven mode relies on large deformation strokes and substantial pre-strain, which limit device miniaturization and energy efficiency. Consequently, increasing attention has turned to torsional deformation as an alternative mode capable of generating large entropy changes at dramatically lower strain levels. Recent studies demonstrate the strong twistocaloric potential of polymeric elastomers. For example, low-crystallinity TPU fibers produced a ΔT_{ad} of −10.2 K under only 50% pre-strain during untwisting, representing a 78.9% improvement over their tensile response. Even without pre-strain, these fibers achieved a twist density of 1.5 turns/mm and a ΔT_{ad} of −8.74 K.[67] Twisted TPE yarns with an effective diameter of 3 mm yielded a temperature drop of approximately −7 K with a twist density of 4 turns·cm^{-1}.[69] Liu *et al.* employed the polybiurea elastomer fiber PpPU2000 with p-phenylene spacers as the twistocaloric refrigerant. By adopting the cooperative working mode of first applying a twist of 3.0 turns·cm^{-1}, then stretching to 350% strain, followed by equilibration and subsequent untwisting prior to strain release, they achieved a maximum cooling temperature drop of −17.1 K, with a corresponding cooling coefficient of performance (COP) of 39.1 and a Carnot efficiency as high as 89.7%. In addition to the large entropy change provided by the soft segments, the nanoknot-like domains in the hard segments offer structural stability, enabling more than 120000 mechanical fatigue life cycles.[70] In addition, supercoiled NR fibers similarly exhibited enhanced cooling performance, reaching −15.5 K at only 100% isometric strain, which surpassed the stretching-release

ΔT_{ad} of −12.2 K at much higher (600%) strain (Fig. 3(c)).[24] The highest COP reached 8.3, highlighting improved energy-conversion efficiency. Simultaneously, scaling the system by untwisting a seven-fiber bundle (diameter 2.2 mm) further increased the surface temperature drop to −19.1 K. When untwisting was combined with tensile unloading, the maximum cooling increased to −16.4 K with a specific cooling energy of 19.4 J·g^{-1}. Also, a cylindrical NR specimen (5 mm diameter, 50 mm mid-section length) achieved a ΔT_{ad} of −41.3 K and a cooling energy of 105.3 J.[71] Collectively, these results highlight that torsional deformation offers a more compact, energy-efficient, and mechanically stable route for elastomer-based flexible solid-state cooling.

2.3. Other polymers

Several different categories of polymers, including ferroelectric polymers, rigid-chain polymers, and spin-crossover (SCO) composites, have recently demonstrated promising elastocaloric and twistocaloric cooling effects, further expanding the material landscape for flexible solid-state refrigeration.[72]

Ferroelectric polymers, such as polyvinylidene fluoride (PVDF), generate cooling via a strong coupling between mechanical deformation, dipole polarization, and structural reorganization.[73] Mechanical deformation of PVDF induces phase transitions from α to β, accompanied by chain alignment and free-volume modification, which collectively drive entropy changes.[74] The PVDF film achieved a ΔT_{ad} of −1.8 K under 15 MPa at 298 K. In addition to tensile loading, untwisting the PVDF fiber at a twist density of 5.0 turns·cm^{-1} produced a ΔT_{ad} of −1.1 K (Fig. 3(d)).[28]

For the first time, the Liu group identified a twistocaloric effect in poly(p-phenylene-2,6-benzobisoxazole) (PBO) fibers, where the intrinsic rigidity and high chain orientation facilitate stress-induced molecular rearrangement and crystalline evolution during torsion. Under a twist density of 7 turns·cm^{-1}, PBO fibers achieved a temperature drop of −1.3 K, illustrating that highly rigid polymer systems undergo entropy-driven cooling under torsional deformation.[29]

In addition, spin-crossover (SCO) polymer composites provide yet another pathway to mechanical cooling through spin-state entropy modulation.[75] Specifically, external mechanical stress triggers a reversible transition between high-spin and low-spin states, yielding spin entropy changes and corresponding temperature variations under adiabatic conditions.[76] For example, polyvinyl chloride (PVC) composite films embedded with $\langle Fe(L)_2\rangle(BF_4)_2$ microcrystals ($L = 2$, 6-bis(pyrazol-1-yl) pyridine), achieved an isothermal entropy change of up to 3.1 J·kg^{-1}·K^{-1} under only 8 MPa and 0.3% strain.[30]

Table 1. Comparison of cooling strategy, cooling temperature, COP, cycle life, cycling cooling temperature among different cooling materials.

Cooling materials	Cooling strategy	Cooling temperature (K)	COP	Cycle life (time)	Cycling cooling temperature (K)	Ref.
$Ni_{52.6}Ti_{47.4}$ wire	Twist	–14.3	30.8	14,752	–3.0	[33]
$Co_{49}Ni_{21}Ga_{30}$ microwire	Stretch	–4.1	–	100	–3.3	[59]
$Cu_{71}Al_{18}Mn_{11}$ microwire	Stretch	–5.0	–	275	–3.0	[57]
$Ni_{50.75}Ti_{48.74}$ wire	Bend	–11.3	21.7	–	–	[41]
$Cu_{71.1}Al_{17.2}Mn_{11.7}$ microwire	Stretch	–11.9	–	200	–5.6	[58]
$Ni_{52.6}Ti_{47.4}$ rod	Twist	–15.0	–	–	–	[40]
$Ni_{50.8}Ti_{49.2}$ spring	Twist and stretch	–16.8	–	1,505	–14.3	[39]
$Ni_{50}Ti_{50}$ wire	Stretch	–17.0	11.8	–	–	[38]
$Ni_{52.6}Ti_{47.4}$ wire	Twist	–17.0	8.3	1,000	∼ −14.5	[24]
NinjaFlex TPU fiber	Stretch	–5.6	3.2	1,000	–	
Ultimaker95A TPU fiber	Stretch	–2.0	1.0	–	–	[68]
Z-Flex TPU fiber	Stretch	–2.8	3.0	–	–	
PVDF fiber	Twist and stretch	–3.0	8.8	2,000	–1.0	[28]
PE- MDI TPU fiber	Stretch	–5.7	–	70	–3.0	[67]
	Twist	–10.2	–	100	∼ −4.0	
self-coiled PBO fiber	Twist and stretch	∼ −4.0	5.8	200,000	∼ −2.0	[29]

Table 1 provides a summary and comparison of key cooling performance for a diverse range of flexible solid-state cooling materials, including shape memory alloys (e.g., NiTi-based, Cu-based alloys) and polymers (e.g., TPU, PVDF, PBO) under various driving modes. Notably, twistocaloric strategies, particularly in NiTi wires, have achieved exceptional energy efficiency (with a COP up to 30.8) and superior cyclic stability (exceeding 14752 cycles), significantly outperforming many conventional uniaxial tensile modes. To visually assess the competitive advantages of various flexible refrigeration materials, Ashby diagrams are shown in Fig. 4. Figure 4(a) demonstrates that torsional loading modes exhibit a significant advantage in enhancing energy conversion efficiency compared to traditional uniaxial stretching. Additionally, hybrid loading modes, such as the combination of twisting and stretching, maintain a desirable system efficiency while achieving a large temperature span by redistributing mechanical stress. Figure 4(b) reveals the critical trade-off be-

tween cooling performance and fatigue life. Torsional deformation generates a nonlinear radial stress gradient that effectively mitigates macroscopic stress concentration and suppresses micro-crack initiation, thereby significantly extending the cyclic reliability of the materials. For instance, NiTi alloys driven by twisting can operate stably for over 14752 cycles, whereas those under tensile modes often suffer from rapid performance degradation due to functional fatigue. In short, these results highlight the growing diversity of polymer-based cooling materials, each leveraging distinct molecular mechanisms (dipole reorientation, rigid-chain reorganization, or spin-state transition) to achieve entropy-driven thermal responses. While the cooling magnitudes remain modest compared to those of elastomers or SMAs, these emerging systems reveal new mechanistic avenues and design principles for next-generation solid-state cooling materials.

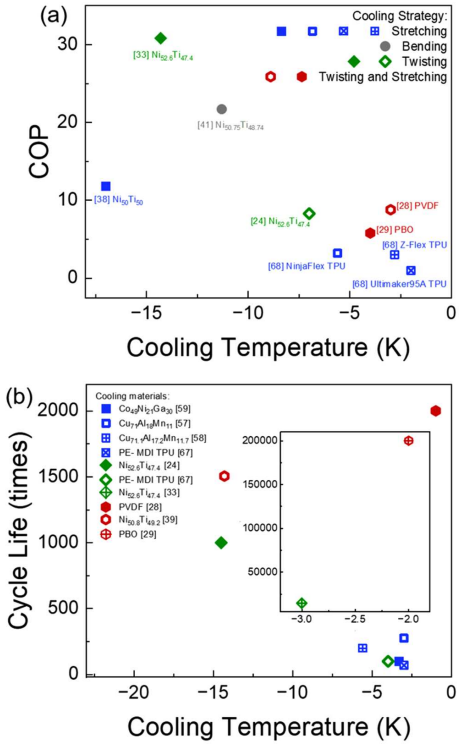


Fig. 4. Comparison of cooling performance and cyclic stability for representative cooling materials. (a) COP as a function of cooling temperature for various materials under different mechanical loading modes, including stretching, bending, twisting, and hybrid twisting-stretching. (b) Cycle life as a function of cooling temperature for diverse cooling materials. The inset highlights the exceptional cyclic stability of PBO fibers and NiTi-based SMAs.

3. Flexible cooling devices

The outstanding performance of flexible cooling materials provides the fundamental basis for solid-state refrigeration, yet material-level properties alone are insufficient to ensure efficient, stable, and durable cooling in practical applications. Device-level design and optimization play an equally critical role, as appropriate architectures and actuation strategies are required to fully activate elastocaloric, twistocaloric, or barocaloric responses while simultaneously enhancing heat-transfer efficiency, energy utilization, and cyclic mechanical reliability. Therefore, building upon advances in flexible cooling materials, this section focuses on the design principles and application strategies of flexible solid-state cooling devices, categorized according to uniaxial stretching, torsional loading, and hybrid deformation modes.

3.1. Uniaxial stretching driven mode

Uniaxial stretching driven cooling devices represent the earliest and most extensively studied category of flexible solid-state cooling applications. However, despite their demonstrated feasibility, their performance remains strongly constrained by heat-transfer limitations, large deformation requirements, and structural inefficiencies.[77] Current research therefore focuses on optimizing device geometry, improving material utilization, and enhancing thermal management to overcome these bottlenecks.

To address heat-management and mechanical-efficiency issues, several groups have explored NiTi-based SMA cooling architectures. Liu *et al.* used an inclined single-motor controlled polycrystalline NiTi wires that were synchronously stretched vertically and translated between a heat source and a heat sink (Fig. 5(a)).[78] The design delivered a ΔT_{ad} of -6.6 K during unloading at 4.8% strain and produced a cooling power of 3.1 W at zero temperature span, which was sufficient for a 0.9-L refrigeration compartment. A roller-driven SMA ribbon device further achieved 78% work-recovery efficiency and a temperature span of 25.4 K by using two oppositely phased $Ti_{49.2}Ni_{44.8}Cu_6$ ribbons working simultaneously (Fig. 5(b)).[79] In addition, topology-optimized structures have been demonstrated to double the heat-transfer efficiency and achieve -15 K cooling of electronic heat flux at least.[80]

Komiya *et al.* established the feasibility of NR-based cooling devices through multichannel tube bundles.[81] By reducing tube diameter and optimizing bundle geometry, they achieved a maximum temperature drop of -8.3 K, with a COP of 6. Later, a miniature NR-foil refrigerator using dual actuators to independently control mechanical loading and thermal contact was developed (Fig. 5(c)).[63] The device achieved a COP of 4.7 and a specific cooling power of 1.1 $W{\cdot}g^{-1}$, though the temperature drop remained modest (≈ -2 K) due to the intrinsically low thermal conductivity of NR (~ 0.15 $W{\cdot}m^{-1}{\cdot}K^{-1}$), which slows heat exchange and limits power density. Therefore, Wang *et al.* introduced a coaxial dual-unit stretching system employing GNS-reinforced SEBS elastomers (Fig. 5(d)), achieving a COP of 8.3 and a temperature span of 3.7 K within 2500 seconds.[82] The coaxial double-unit coupling enabled energy recovery, affording a 56.3% energy-recovery efficiency.

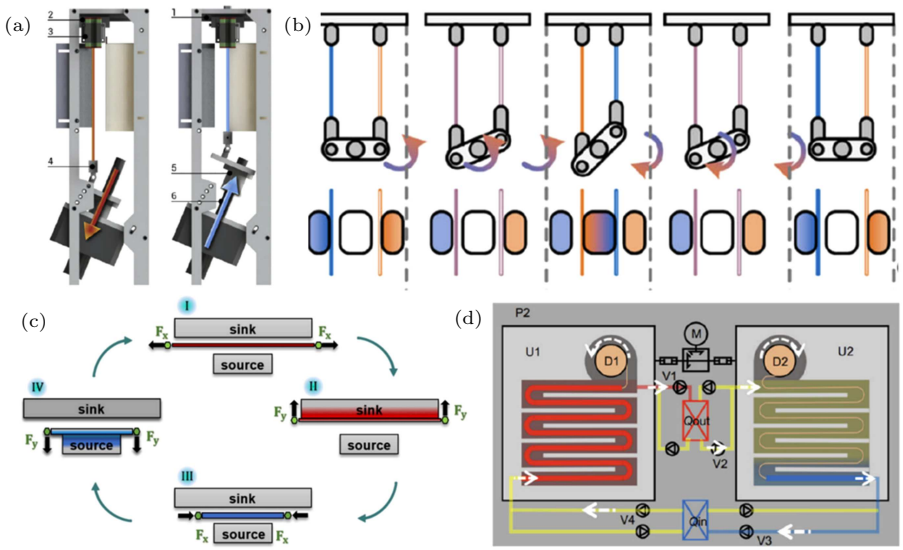


Fig. 5. Compact elastocaloric stretching devices driven by uniaxial tension. (a) A compact heat pump driven by a motor-screw coupling mechanism to control the stretching and reciprocating motion of SMAs. Reproduced with permission from Ref. [78] Copyright 2022 The Innovation Press. (b) Utilizing a crank rod mechanism to induce torsion at both ends of SMA, generating cooling effects during cyclic deformation. Reproduced with permission from Ref. [79] Copyright 2024 Springer Nature. (c) Schematic of flexible NR materials used in thermal contact separation refrigeration cycles. Reproduced with permission from Ref. [63] Copyright 2024 IOP Publishing. (d) A heat pump using an electric motor to stretch SEBS materials and exchange heat with fluids flowing through a serpentine channel. Reproduced with permission from Ref. [83] Copyright 2024 Springer Nature.

3.2. Twisting driven mode

In uniaxial stretching refrigeration, large axial strain and stress concentration limit both mechanical durability and heat-transfer efficiency, motivating the exploration of alternative deformation modes. Twisting loading offers a distinct mechanical pathway in which shear stress dominates the entropy modulation process. Under comparable strain levels, twisting activates more sufficient phase transitions and entropy changes at significantly lower driving stress, while the radial shear-stress gradient and longitudinally uniform deformation help mitigate local stress concentration and facilitate more effective heat exchange.[83]

Multi-strand NiTi wires in twistocaloric refrigerators, for instance, have achieved a water temperature drop of −7.7 K, corresponding to a specific cooling energy of 6.75 $J\cdot g^{-1}$.[24] Importantly, architectural refinements, such as periodic nonlinear stress profiles and physical separation of hot and cold fluid channels, further enhanced performance gains (Fig. 6(a)). In a multi-stage torsional heat-pump configuration (Fig. 6(b)), optimization of twist density and wire length resulted in a water temperature drop of −13.8 K and a cooling power of 5.0 W, with a specific cooling power of 1.2 $W\cdot g^{-1}$ and a system COP of 19.5.[33] Stable operation over more than 2000 cycles indicates that torsional loading can sustain repeated cooling cycles without severe mechanical degradation.

From a design perspective, the twisting-driven mode is particularly suitable for fiber-based flexible cooling devices, as it combines low driving stress with mechanically stable deformation. Its advantages are most pronounced when the deformation geometry, twist density, and thermal management are carefully coordinated. Within these constraints, twistocaloric devices provide a practical route toward compact and scalable solid-state cooling systems, especially in applications where flexibility and cyclic durability are required.

3.3. Hybrid loading driven mode

Hybrid deformation modes have been introduced to address the intrinsic limitations of single-mode elastocaloric loading, particularly the high actuation force and restricted strain utilization associated with pure uniaxial stretching. By combining tensile, torsional, bending, or volumetric deformation, hybrid loading redistributes mechanical stress and enables thermal responses to be activated under reduced external force.[84] At the device level, this approach also allows greater flexibility in geometric design, which can be exploited to improve heat exchange and system compactness, albeit often at the cost of increased structural and control complexity.[85]

Current research demonstrates that hybrid-mode systems not only enhance mechanical efficiency but also enable more effective heat transfer through improved geometric coupling and continuous-flow configurations. A representative example is the coil-bending cooling device developed by Sun *et al.*, in which NiTi ribbons were actuated by rotary motors to realize air cooling without liquid heat exchangers (Fig. 6(c)), affording a temperature drop of −10.6 K, a COP of 3.7, and a specific cooling power of 2.5 $W\cdot g^{-1}$.[86] This architecture eliminated the need for liquid heat exchangers or sealed fluid loops, significantly reducing system size and operational complexity. The low driving force enabled by coil-bending produced a substantial temperature drop in air, while serial and parallel air-channel layouts allowed separate optimization of temperature span and specific cooling power. This work demonstrates

that hybrid bending modes can translate mechanical advantages into functional air-cooling performance, particularly in compact configurations.

Hybrid deformation strategies have also been extended to polymer-based cooling devices. Wang *et al.* reported a rotary-motion cooling device based on SEBS elastomers, in which cyclic stretching, rotation, and intermittent mechanical contact were synchronized to promote heat separation during each cooling cycle (Fig. 6(d)).[62] The coordinated motion improved thermal interface stability and enabled partial energy recovery, resulting in stable cooling operation and measurable temperature differentials in flowing water (a water temperature drop of −3.7 K). These results suggest that hybrid loading can mitigate the slow heat-exchange kinetics commonly encountered in tensile-only polymer devices. In addition, an all-soft elastocaloric heat pump based on thin latex membranes undergoing cyclic inflation and deflation was designed (Fig. 6(e)), which achieved a temperature drop of −7.9 K, a COP of 4.7, and a specific cooling power of 20.9 $W{\cdot}g^{-1}$.[87] The spherical membrane geometry minimized frictional losses and enabled quasi-adiabatic deformation on sub-100 ms timescales, leading to high specific cooling power. This example highlights how unconventional hybrid deformation pathways can leverage instability-driven mechanics to access performance regimes that are difficult to achieve with steady, single-mode loading.

Table 2 summarizes the system-level cooling performance of representative twistocaloric and elastocaloric refrigeration devices driven by linear and non-linear stresses. Notably, NiTi wires utilizing torsional loading achieve superior energy efficiency (with a COP of 19.5), whereas latex membranes demonstrate exceptional specific cooling power (20.9 $W{\cdot}g^{-1}$), illustrating the diverse potential of flexible materials in meeting specific thermal management requirements. Overall, hybrid-mode elastocaloric devices reveal a promising route toward high-performance cooling at low actuation force, offering improved strain utilization, enhanced thermal exchange, and greater architectural freedom compared with single-mode loading schemes. These advantages position hybrid deformation strategies as an important bridge between material-level elastocaloric effects and practical, compact solid-state refrigeration technologies.

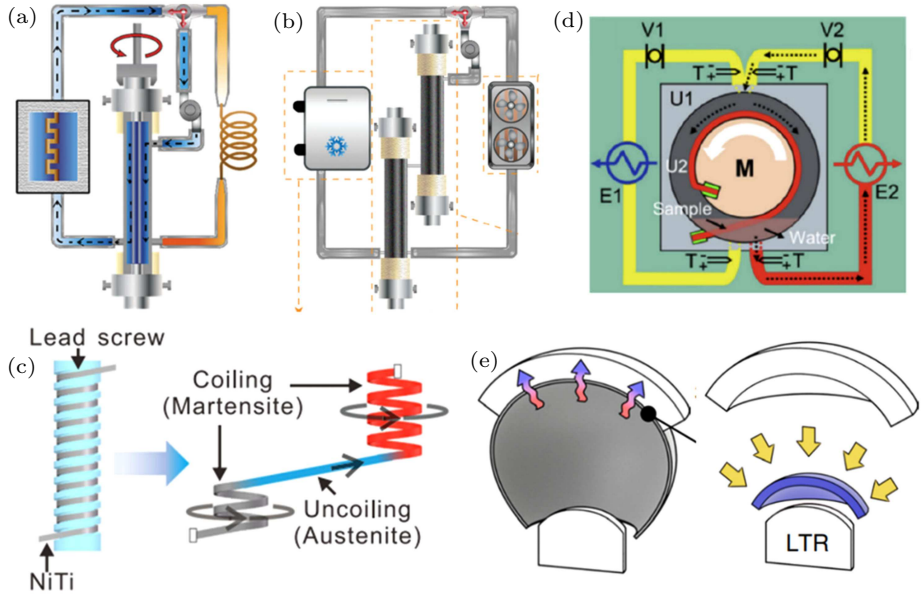


Fig. 6. Cooling devices driven by periodic torsional stress and other hybrid driven modes. (a) Schematic of a twistocaloric cooling system realizing the alternating switching of cold and hot fluids through a three-way valve. (b) Schematic of a multi-stage twistocaloric device with serially connected modules. Reproduced with permission from Ref. [33] Copyright 2024 Wiley-VCH. (c) Compact cooling unit with coiled NiTi ribbons under torsional and bending loading modes. Reproduced with permission from Ref. [86] Copyright 2023 Springer Nature. (d) The SEBS elastomer rotary motion cooling device achieved thermal separation through stretching, rotation and mechanical contact. Reproduced with permission from Ref. [62] Copyright 2022 Springer Nature. (e) membrane-based elastocaloric refrigerator operated in mechanical contact with heat sink and heat source, illustrating the temperature decrease during adiabatic contraction. Reproduced with permission from Ref. [87] Copyright 2021 Springer Nature.

Table 2. Summary of the cooling materials driven by non-linear stress and linear stress used for twistocaloric and elastocaloric refrigeration, involving heat exchange medium, ΔT_{drop} of device, COP_{sys}, specific cooling power.

Cooling materials	Heat exchange medium	ΔT_{drop} of device (K)	COP	SCP ($W{\cdot}g^{-1}$)	Ref.
$Ni_{52.6}Ti_{47.4}$ wire	Water	−13.8	19.5	1.2	[33]
NiTi ribbon	Air	−10.6	3.7	2.5	[86]
Latex membrane	Mechanical contact	−7.9	4.7	20.9	[87]
TPEs-1 SEBS film	Water	−1.1	9.3	1.9	[82]
GNS-SEBS	Mechanical contact	−3.7	8.3	–	[62]
Natural rubber tube	Air	−8.3	6.0	0.14	[81]
Natural rubber foil	Mechanical contact	−4.1	4.7	1.1	[63]

4. Conclusion and future perspective

In this review, we have systematically summarized recent advances in flexible solid-state caloric cooling, with a focus on high-performance materials and device architectures driven by diverse mechanical loading modes: uniaxial stretching, pure twisting, and hybrid deformation. We have detailed the molecular- and microstructure-level mechanisms, including martensite phase transitions in SMAs, entropy-driven chain alignment in elastomeric polymers, and novel entropy modulations in other polymer systems.

The core findings highlight that torsional deformation provides a structurally and energetically efficient pathway for both SMAs and elastomers, enabling large adiabatic temperature changes under dramatically lower driving stress, which significantly enhances the material's fatigue life and the system's COP. Concurrently, hybrid loading modes further expand the design freedom, offering enhanced heat transfer and energy recovery compared to single-mode systems. The development of corresponding cooling devices across uniaxial, twisting, and hybrid modes has demonstrated the feasibility of highly integrated, flexible, and efficient thermal management systems.

Despite significant progress, several key challenges must be addressed to transition flexible solid-state cooling technologies from lab prototypes to large-scale commercial applications. The future development of flexible cooling technology will rely on the synergistic advancement of materials science, device engineering, and interdisciplinary integration.[88–93]

The future advancement of flexible cooling technology will critically depend on the exploration and optimization of high-performance flexible materials. The integration of emerging material systems, such as nanomaterials and composite materials, is expected to significantly enhance the thermal response rate, durability, and mechanical properties of flexible cooling materials. The construction of novel gradient and hierarchical structures can effectively reduce thermal hysteresis and improve energy conversion efficiency. Moreover, the development of sustainable and cost-effective flexible cooling materials has garnered increasing attention. The adoption of bio-based polymers and recyclable high-molecular-weight materials is anticipated to mitigate environmental impact and lay the foundation for the large-scale application of flexible cooling technologies in sustainable energy systems.

Further progress in flexible cooling systems necessitates a focus on achieving larger cooling temperature differences and enhancing long-term operational stability. Optimizing the thermal conductivity and phase transition properties of materials to achieve greater adiabatic temperature changes is essential for improving cooling capacity. Additionally, the long-term stability of flexible cooling materials under prolonged cyclic loading with large strain amplitudes remains a challenge, requiring further improvements to prevent degradation-induced efficiency loss. Moreover, adaptability to diverse environmental conditions and the ability to meet various application demands impose higher requirements on flexible cooling technologies. These include maintaining high-performance cooling under different temperature and humidity conditions and ensuring applicability in wearable devices and microelectronic cooling systems.

The future development of flexible cooling technologies will heavily rely on interdisciplinary integration, promoting their convergence with other advanced thermal management strategies to further enhance overall system efficiency and expand the operational temperature range. The incorporation of intelligent sensing and adaptive control systems will enable intelligentization and precise thermal regulation of flexible cooling devices. Furthermore, in specialized application scenarios such as healthcare and aerospace, flexible cooling systems can be integrated with bio-thermal management and phase-change energy storage technologies to provide more competitive solutions for temperature control under extreme environmental conditions.

Acknowledgements

This work was supported by the National Natural Science Foundation of China (Grant Nos. 52225306, 52550003, 52350120, 52090034, 52461160302, 51973093, 51773094 and 22371300), the National Key Research and Development Program of China (Grant No. 2022YFB3807103), Frontiers Science Center for New Organic Matter, Nankai University (Grant No. 63181206), the Fundamental Research Funds for the Central Universities (Grant No. 63171219), Beijing–Tianjin–Hebei Basic Research Cooperation Project (Grant No. J230023), Tianjin Science and Technology Program (Grant Nos. 25JCYBJC01420, 23JCZDJC00880, and 22JCYBJC01260), and Anhui Provincial Science and Technology Innovation Tackling Program (Grant No. 202423i08050057). We thank the Shanghai Synchrotron Radiation Facility of BL16B1 (https://cstr.cn/31124.02.SSRF.BL16B1) for the assistance on WAXS and SAXS measurements. Work at the University of Texas at Dallas was supported by a Robert A. Welch Foundation grant (AT-0029).

References

[1] Alahmer A, Wang X and Alam K C A 2020 *Energies* **13** 1005
[2] Llopis R, Nebot-Andrés L, Sánchez D, Catalán-Gil J and Cabello R 2018 *Int. J. Refrig.* **93** 85
[3] Alajmi A and Zedan M 2020 *Sustainable Cities and Soc.* **54** 101976
[4] Isaac M and Vuuren D P 2009 *Energy Policy* **37** 507
[5] Giulia U, Gianluca R, Florian B, Riccardo P, Francesco F, Shamila H, Manfred K and Mat S 2019 *AIMS Materials Science* **6** 1135
[6] Domanski P A, Steven Brown J, Heo J, Wojtusiak J and McLinden M O 2014 *Int. J. Refrig.* **38** 71

[7] Moya X and Mathur N D 2020 *Science* **370** 797
[8] Mañosa L and Planes A 2020 *Appl. Phys. Lett.* **116** 050501
[9] Starkov A, Pakhomov O and Starkov I 2012 *Ferroelectrics* **430** 108
[10] Qin Y X, Qin B C, Wang D Y, Chang C and Zhao L D 2022 *Energy Environ. Sci.* **15** 4527
[11] Ziabari A, Zebarjadi M, Vashaee D and Shakouri A 2016 *Rep. Prog. Phys.* **79** 095901
[12] Tregnago G 2023 *Nat. Energy* **8** 640
[13] Fan X, Chen S, Manshaii F, Duan Z, Chen G, Zhao X, Zhou Y and Chen J 2026 *Adv. Funct. Mater.* **36** 2420997
[14] Zhang J R, Xu Y X, An S H, Sun Y, Li X D and Li Y C 2020 *Chin. Phys. B* **29** 076202
[15] Ossmer H and Kohl M 2016 *Nat. Energy* **1** 16159
[16] Qian S, Geng Y, Wang Y, Ling J, Hwang Y, Radermacher R, Takeuchi I and Cui J 2016 *Int. J. Refrig.* **64** 1
[17] Frenzel J, Eggeler G, Quandt E, Seelecke S and Kohl M 2018 *MRS Bull.* **43** 280
[18] Lu B and Liu J 2015 *Sci. Bull.* **60** 1638
[19] Wang S, Shi Y, Li Y, Lin H, Fan K andTeng X 2023 *Renew Sust. Energ Rev.* **187** 113762
[20] Mevada H, Liu B, Gao L, Hwang Y, Takeuchi I and Radermacher R 2024 *Int. J. Refrig.* **162** 86
[21] Imran M and Zhang X 2020 *Mater. Des.* **195** 109030
[22] Elahinia M H, Hashemi M, Tabesh M and Bhaduri S B 2012 *Prog. Mater. Sci.* **57** 911
[23] Coativy G, Haissoune H, Seveyrat L, Sebald G, Chazeau L, Chenal J M and Lebrun L 2020 *Appl. Phys. Lett.* **117** 193903
[24] Wang R, Fang S L, Xiao Y C, *et al*. 2019 *Science* **366** 216
[25] Hartquist C M, Lin S, Zhang J H, Wang S, Rubinstein M and Zhao X 2023 *Sci. Adv.* **9** eadj0411
[26] Zhou X, Fang S, X. Leng, Liu Z and Baughman R H 2021 *ACC Chem. Res.* **54** 2624
[27] Zhang Y, Yu C, Song D, Zhu Y, Kan Q and Kang G 2023 *Mech. Mater.* **178** 104575
[28] Wang R, Zhou X, Wang W and Liu Z 2021 *Chem. Eng. J.* **417** 128060
[29] Feng D, Xiao Y, Wang G, Mei G, Guo W, Yu K, Liu S, Zhao W, Zhou X and Liu Z 2023 *Macromol. Rapid Commun.* **44** 2300318
[30] Lünser K, Kavak E, Gürpinar K, Emre B, Atakol O, Stern-Taulats E, Porta M, Planes A, Lloveras P, Tamarit J L and Mañosa L 2024 *Nat. Commun.* **15** 6171
[31] McConnon A 2021 *Scilight* **2021** 111105
[32] Engelbrecht K 2019 *J. Phys. Energy* **1** 021001
[33] Xiao Y, Mei G, Feng D, Zhao W, Guo W, Leng X, Qian D, Zhao W, Bai J, Wang Z, Zhu M, Zhou X and Liu Z 2024 *Adv. Mater.* **36** 2407009
[34] Li L, He S, Xiao F, Zeng Y, Liu Y, Zhou Y, Cai X and Jin X 2025 *Prog. Mater. Sci.* **153** 101477
[35] Li X, Hua P and Sun Q 2023 *Nat. Commun.* **14** 7982
[36] Chen J, Lei L and Fang G 2021 *Mater. Today Commun.* **28** 102706
[37] Soto-Parra D, Vives E, Mañosa L, Matutes-Aquino J A, Flores-Zúñiga H and Planes A 2016 *Appl. Phys. Lett.* **108** 071902
[38] Cui J, Wu Y, Muehlbauer J, Hwang Y, Radermacher R, Fackler S, Wuttig M andTakeuchi I 2012 *Appl. Phys. Lett.* **101** 073904
[39] Zhu X, Zhang X, Qian M, Zhong S, Muhammad I and Geng L 2022 *Mater. Sci. Eng. A* **838** 142787
[40] Zheng J, Li Z, Lv C, Li G, Wang B, Zhang K, Bao R, Gan B, Zhao X and Hou H 2024 *J. Phys. D Appl. Phys.* **58** 075503
[41] Sharar D J, Radice J, Warzoha R, Hanrahan B and Smith A 2021 *Appl. Phys. Lett.* **118** 184103
[42] Tušek J, Žerovnik A, Čebron M, Brojan M, Žužek B, Engelbrecht K and Cadelli A 2018 *Acta Mater.* **150** 295
[43] Chen J, Yin H and Sun Q 2020 *Acta Mater.* **195** 141
[44] Chen J, Lei L and Fang G 2022 *J. Alloys Compd.* **927** 166951
[45] Hua P, Xia M, Onuki Y and Sun Q 2021 *Nat. Nanotechnol.* **16** 409
[46] Xu B, Wang C, Wang Q, Yu C, Kan Q and Kang G 2023 *Int. J. Mech. Sci.* **246** 108140
[47] Sun X, Xie C, Chen S, Wan J, Tan G and Tang X 2024 *Chin. Phys. B* **33** 057201
[48] Zhou M, Wang W, Su H, Hu Z and Li L 2024 *Chin. Phys. B* **33** 056501
[49] Chen J, Xing L, Fang G, Lei L and Liu W 2021 *Acta Mater.* **208** 116741
[50] Chen J, Zhao C, Zhang S, Zhang W, Liu W, Lei L, Ramamurty U and Fang G 2024 *Mater. Sci. Eng. A* **892** 146073
[51] Chluba C, Ge W, Lima de Miranda R, Strobel J, Kienle L, Quandt E and Wuttig M 2015 *Science* **348** 1004
[52] Zhang H, Liu J, Ma Z, Ren Y, Jiang D, Cui L and Yu K 2022 *J. Alloys Compd.* **928** 167195
[53] Hou, H, Simsek E, Ma T, *et al*. 2019 *Science* **366** 1116
[54] Wang Y, Du H, Liu H, Yang J, Li Z, Li J, Yang B, Yan H and Zuo L 2024 *Scr. Mater.* **252** 116227
[55] Moya X, Defay E, Heine V and Mathur N D 2015 *Nat. Phys.* **11** 202
[56] Wang Y, Liu C, Wang H, Li Z, Li J, Yang B, Yan H and Zuo L 2024 *Scr. Mater.* **246** 116092
[57] Yuan B, Qian M, Zhang X, Imran M and Geng L 2020 *Int. J. Refrig.* **114** 54
[58] Yuan B, Zhong S, Qian M, Zhang X and Geng L 2021 *J. Alloys Compd.* **850** 156612
[59] Zhang X, Xu N, Yang J, Niu Y, Cao Y, Cong D, Chen H and Wang Y D 2024 *Mater. Lett.* **362** 136165
[60] Torello A and Defay E 2022 *Chem* **8** 3165
[61] Guyomar D, Li Y, Sebald G, Cottinet P J, Ducharne B and Capsal J F 2013 *Appl. Therm. Eng.* **57** 33
[62] Zhang S, Yang Q, Li C, Fu Y, Zhang H, Ye Z, Zhou X, Li Q, Wang T, Wang S, Zhang W, Xiong C and Wang Q 2022 *Nat. Commun.* **13** 9
[63] Ludwig C, Leutner J, Prucker O, Rühe J and Kohl M 2024 *J. Phys. Energy* **6** 015009
[64] Candau N, Vives E, Fernández A I and Maspoch M L 2021 *Polymer* **236** 124309
[65] Haissoune H, Coativy G, Chazeau L, Lebrun L, Sebald G and Chenal J M 2024 *Polymer* **307** 127234
[66] Zhang S, Fu Y, Li C, Nie X, Chen J, Zhou Y, Ye Z, Zhou X, Shu B, Xiong C, Yang Q and Wang Q 2022 *Cell Rep. Phys. Sci.* **3** 101147
[67] Zhang J, Wu Y, Lv Y, Zhu G and Zhu Y 2024 *Polymers* **16** 3360
[68] Wang K, Engelbrecht K and Bahl C R H 2023 *Appl. Mater. Today* **30** 101711
[69] Mei G, Li J, Feng D, Qian D and Liu Z 2023 *Macromol. Rapid Commun.* **44** 2300275
[70] Li J, *et al*. 2026 *Adv. Mater.* **38** e16934
[71] Liu B, Wang Y, Zhu Z, Theodorakis P E, Song J and Bennacer R 2023 *Int. J. Refrig.* **155** 163
[72] Cazorla C 2019 *Appl. Phys. Rev.* **6** 041316
[73] Zhang Y, Zhang S, Ye Z, Niu F, Fu Y, Qin H, Xiong C, Yang Q and Wang Q 2025 *Chem. Eng. J.* **524** 169794
[74] Patel S, Chauhan A, Vaish R and Thomas P 2016 *Appl. Phys. Lett.* **108** 072903
[75] Seo J, Braun J D, Dev V M and Mason J A 2022 *J. Am. Chem. Soc.* **144** 6493
[76] Robb M G and Boström H L B 2025 *Dalton Trans.* **54** 10935
[77] Schmidt M, Schütze A and Seelecke S 2016 *APL Mater.* **4** 064107
[78] Chen Y, Wang Y, Sun W, Qian S and Liu J 2022 *The Innovation* **3** 100205
[79] Yao S, Dang P, Li Y, Wang Y, Zhang X, Liu Y, Qian S, Xue D and He Y L 2024 *Nat. Commun.* **15** 7203
[80] Dong X, Jiang X and Li P 2025 *Appl. Therm. Eng.* **265** 125509
[81] Sebald G, Lombardi G, Coativy G, Jay J, Lebrun L and Komiya A 2023 *Appl. Therm. Eng.* **223** 120016
[82] Zhang S, Yang Q, Li C, Fu Y, Zhang H, Ye Z, Zhou X, Li Q, Wang T, Wang S, Zhang W, Xiong C and Wang Q 2024 *Nat. Commun.* **15** 6567
[83] Zhao H and Wu K 2022 *PLOS One* **17** e0277415
[84] Li X, Cheng S and Sun Q 2022 *Appl. Therm. Eng.* **215** 118942
[85] Cheng S, Sun W, Li X and Zhang J 2024 *APL Mater.* **12** 081116
[86] Li X, Hua P and Sun Q 2023 *Nat. Commun.* **14** 7982
[87] Greibich F, Schwödiauer R, Mao G, Wirthl D, Drack M Baumgartner R, Kogler A, Stadlbauer J, Bauer S, Arnold N and Kaltenbrunner M 2021 *Nat. Energy* **6** 260
[88] Zhou G, Zhang L, Li Z, Hua P, Sun Q and Yao S 2025 *Nature* **639** 87
[89] Qian S, Catalini D, Muehlbauer J, Liu B, Mevada H, Hou H, Hwang Y, Radermacher R and Takeuchi I 2023 *Science* **380** 722
[90] Defay E 2025 *Joule* **9** 101960
[91] Cai J, Yang B and Akbarzadeh A 2024 *ACS Nano* **18** 894
[92] Hirai T, Iguchi R, Miura A and Uchida K 2022 *Adv. Funct. Mater.* **32** 2201116
[93] Xu B, Xiong J, Yu C, Wang C, Wang Q and Kang G 2022 *Int. J. Mech. Sci.* **222** 107256